CIRCUIT ANALOG TECHNIQUES FOR ANALYSIS OF RESONANTLY-COUPLED LINEAR ACCELERATOR STRUCTURES*

G. R. Swain
Los Alamos Scientific Laboratory
Los Alamos, New Mexico

Introduction

One approach to the study of the expected performance of proposed accelerator structures employs a direct analysis of the fields produced therein. For simple accelerator structures, such as the Alvarez configuration and the iris-loaded waveguide, analysis of the coupled fields is possible, usually with the aid of a few simplifying approximations. The dispersion relation[1] and even the transient response[2] have been obtained in this way. On the other hand, a circuit analog can permit one to investigate the expected performance of a structure without having to investigate the detailed configuration of the fields. The circuit analog is capable of giving insight to the nature of the dispersion relation,[3] the optimum tuning of the individual cells,[4] the amount of degradation in performance to be expected from tuning errors or other errors,[5] and the expected performance under a given set of operating conditions.[6] These capabilities have proved very useful at Los Alamos, where side-coupled and cloverleaf accelerator structures have been under study. A number of relations between the field approach and the circuit analog approach have been worked out, but with certain assumptions regarding the nature of the coupling between the cavities.[7] The application of the circuit analog to the study of resonantly-coupled accelerator structures will be discussed in this paper.

Notation

A circuit analog for a chain of N+1 cavities or cells (which includes N/2 coupling cavities) is shown in Fig. 1. With mutual impedance terms between inductors r and s expressed in the form

$$M_{rs} = k_{r,s}\sqrt{L_r L_s}\ ,$$

The circuit equations may be written

$$E_n = \left(2j\omega L_n + \frac{1}{j\omega C_n} + R_n\right) W_N(n)\ I_n$$
$$+ j\omega\sqrt{L_n}\left(k_{n-1,n}\sqrt{L_{n-1}}\ I_{n-1} + k_{n,n+1}\sqrt{L_{n+1}}\ I_{n+1}\right)$$
$$+ j\omega\sqrt{L_n}\left(k_{n-2,n}\sqrt{L_{n-2}}\ I_{n-2} + k_{n,n-2}\sqrt{L_{n+2}}\ I_{n+2}\right),$$
$$n = 0, 1, 2, \cdots, N \qquad (1)$$

The terms in the second set of parentheses represent near-neighbor coupling; the terms in the third set, next nearest neighbor coupling. The latter is designated direct coupling, since it is coupling directly between accelerating cells or between coupling cells. A factor $W_N(n)$ is necessary to account for the end cell configuration:

$$W_N(n) = 1, \quad n = 1, 2, \cdots, N-1$$
$$= \tfrac{1}{2}, \quad n = 0, N.$$

An alternative notation uses quantities proportional to energy brought in or stored:

$$Y_n^2 = \frac{E_n^2}{L_n}\left[W_N(n)\right]^{-2} = \text{energy drives}$$

$$X_n^2 = I_n^2 L_n = \text{stored energy responses}$$

$$\omega_{in} = \left(2\ L_n C_n\right)^{-\frac{1}{2}} = \text{individual resonant frequencies}$$

and

$$Q_n = 2\omega_{in} L_n / R_n = \text{quality factors.}$$

Then the circuit equations may be written

$$X_n + \frac{1}{2W_N(n)}\left(k_{n-1,n}\ X_{n-1} + k_{n,n+1}\ X_{n+1}\right)$$
$$+ \frac{1}{2W_N(n)}\left(k_{n-2,n}\ X_{n-2} + k_{n,n+2}\ X_{n+2}\right)$$
$$+ j\ \frac{1}{2\omega}\ Y_n = \left(\frac{\omega_{in}}{\omega}\right)^2 X_n + j\left(\frac{\omega_{in}}{\omega Q_n}\right) X_n,$$
$$n = 0, 1, 2, \cdots, N. \qquad (2)$$

For the purpose of direct numerical solution, it is convenient to represent the N+1 equations (2) by the single matrix equation

$$\hat{M}_T\ \vec{X} = -j\ \frac{1}{2\omega}\ \vec{Y} \qquad (3)$$

where X_n and Y_n are the components of $\vec{X}$ and $\vec{Y}$, and

$$\hat{M}_T = \begin{pmatrix} Z_0 & k_{0,1} & k_{0,2} & 0 & \cdots & 0 \\ \tfrac{1}{2}k_{0,1} & Z_1 & \tfrac{1}{2}k_{1,2} & \tfrac{1}{2}k_{2,3} & & \\ \tfrac{1}{2}k_{0,2} & \tfrac{1}{2}k_{1,2} & Z_2 & \tfrac{1}{2}k_{1,3} & & \\ 0 & \tfrac{1}{2}k_{1,3} & \tfrac{1}{2}k_{2,3} & Z_3 & & \\ 0 & \cdots & & & & Z_N \end{pmatrix},$$

in which $Z_n = 1 - \left(\frac{\omega_{in}}{\omega}\right)^2 - j\left(\frac{\omega_{in}}{\omega Q_n}\right)$.

For the purpose of error analysis, it is

* Worked performed under the auspices of the U. S. Atomic Energy Commission.

convenient to represent the N+1 equations (2) by the matrix equation

$$\left(\hat{M} + \hat{M}_D - \lambda\hat{E} - \lambda\hat{F} - j\hat{L}\right)\vec{X} + j\frac{1}{2\omega}\vec{Y} = \left(\lambda + j\alpha\right)\vec{X}, \tag{4}$$

where $\vec{X}$ and $\vec{Y}$ are as above and where the meanings of the other symbols are explained below:

$$\hat{M} = \begin{pmatrix} 1 & k & 0 & \cdots & 0 \\ \frac{1}{2}k & 1 & \frac{1}{2}k & & \\ 0 & \frac{1}{2}k & 1 & & \\ \cdots & & & \cdots & \\ 0 & & & & 1 \end{pmatrix} \tag{5}$$

$$\hat{M}_D = \begin{pmatrix} 0 & \left(k_{o,1}-k\right) & k_{o,2} & \cdots & 0 \\ \frac{1}{2}\left(k_{o,1}-k\right) & 0 & \frac{1}{2}\left(k_{1,2}-k\right) & & \\ \frac{1}{2}k_{o,2} & \frac{1}{2}\left(k_{1,2}-k\right) & 0 & & \\ \cdots & & & \cdots & \\ 0 & & & & \end{pmatrix} \tag{6}$$

Matrix $\hat{M}$ contains the near-neighbor coupling strengths desired while $\hat{M}_D$ contains any variation from these desired strengths plus any direct coupling coefficients present. The frequency ratio terms on the right side of (2) have been split into constant and varying parts as follows:

$$\left(\frac{\omega_{in}}{\omega}\right)^2 = \lambda + \lambda\Delta_n + \lambda\epsilon_n \tag{7}$$

$$\left(\frac{\omega_{in}}{\omega Q_n}\right) = \alpha + \psi_n \tag{8}$$

where

$$\lambda = \left(\frac{\omega_i}{\omega}\right)^2 \qquad \Delta_n = \frac{\omega_{an}^2 - \omega_i^2}{\omega_i^2} \qquad \epsilon_n = \frac{\omega_{in}^2 - \omega_{an}^2}{\omega_i^2}$$

$$\alpha = \left(\frac{\omega_i}{\omega Q_i}\right) \qquad \psi_n = \frac{\omega_{in}}{\omega Q_n} - \frac{\omega_i}{\omega Q_i}$$

The diagonal elements of the diagonal matrices $\hat{E}$, $\hat{F}$, and $\hat{L}$ in (4) are formed by the ϵ_n, the Δ_n, and the ψ_n respectively. The constant Q_i is the average Q desired. The constant ω_i is the desired frequency for the $\pi/2$-mode. (If direct coupling is not present, all cells should be tuned as closely as possible to ω_i.) The cell-to-cell variations present in any actual structure are represented by Δ_n, ϵ_n, and ψ_n. The quantities Δ_n represent any deliberate frequency adjustments, while the quantities ϵ_n represent uncontrolled variations such as tuning errors.

The need to make deliberate frequency shifts for the different cells arises in the following way. In order to achieve maximum mode separation and to provide a near-optimum condition for power transfer down a biperiodic structure operated in the $\pi/2$-mode, the stop band in the dispersion characteristic should be eliminated. In order to eliminate the stop band for a structure with direct coupling present, offsets in the desired individual cell frequency ω_{an} are required. These frequency offsets will be represented by the Δ_n. An equation specifiying the Δ_n will be given in the following section.

Relation of Error Analysis With Direct Coupling Present to the Analysis Without Direct Coupling

If the direct coupling coefficients, the frequency offsets, frequency and coupling errors, and losses (and consequently drives) are made to approach zero in (4), what remains is

$$\hat{M}\vec{X} = \lambda\vec{X}, \tag{9}$$

a classical eigenvalue (λ) eigenvector ($\vec{X}$) problem specification. It may be verified that (9) is satisfied by the complete set of eigenvectors

$$\vec{X} = \vec{X}_R, \quad R = 0, 1, 2, \cdots, N,$$

where the components of $\vec{X}_R$ are given by

$$X_{Rn} = \cos\frac{\pi nR}{N}, \tag{10}$$

provided that

$$\lambda_R = \left(\omega_i/\omega_R\right)^2 = 1 + k\cos\frac{\pi R}{N}.$$

When investigating the effects of losses or errors in (4), it is advantageous to expand $\vec{X}$ as a series in the $\vec{X}_R$, since then the relation

$$\hat{M}\vec{X}_R = \lambda_R\vec{X}_R$$

can be used.

If the effect of tuning errors for the case with low losses and without direct coupling is to be investigated, then $\vec{X}$, the solution for a given mode P, may be set equal to a constant times the P-mode solution to (9) plus a perturbation, $\delta\vec{X}$:

$$\vec{X} = A_P\vec{X}_P + \vec{\delta X}. \tag{11}$$

The resulting equation for $\vec{\delta X}$, since no frequency offsets are necessary, is[5]

$$\left(\hat{M} - \lambda_P\hat{E}\right)\vec{\delta X} - A_P\lambda_P\hat{E}\vec{X}_P = \lambda_P\vec{\delta X}. \tag{12}$$

Similarly, if the effect of tuning errors for the case with low losses and with direct coupling present is to be studied, $\vec{X}$ may again be expressed

$$\vec{X} = A_P\vec{X}_P + \vec{\delta X}.$$

The resulting equation for $\vec{\delta X}$ is then

$$\left(\hat{M} + \hat{M}_D - \lambda_P\hat{E} - \lambda_P\hat{F}\right)\vec{\delta X} + \left(\hat{M}_D - \lambda_P\hat{E} - \lambda_P\hat{F}\right)A_P\vec{X}_P = \lambda_P\vec{\delta X} \qquad (13)$$

In order to achieve a solution $\vec{X}$ with direct coupling present that behaves like the solution $\vec{X}_P$ obtained with no direct coupling (i.e., to achieve a solution $\vec{X}$ with no stop band), it is required that (13) be satisfied in the absence of errors. For $\vec{\delta X} = 0$, $\hat{E} = 0$, the required condition is

$$\hat{M}_D\vec{X}_P = \lambda_P\hat{F}\vec{X}_P. \qquad (14)$$

Since $\hat{F}$ is a diagonal matrix, it is a simple matter to solve for the necessary frequency offsets:

$$\Delta_n = \frac{\sum_{r=o}^{N} M_{Dn,r}\cos\frac{\pi rP}{N}}{\lambda_P\cos\frac{\pi nP}{N}}.$$

For an infinitely long biperiodic structure with uniform nearest-neighbor coupling operated in the $\pi/2$-mode, for example,

$$\Delta_n = -\tfrac{1}{2}\left(k_{n-2,n} + k_{n,n+2}\right).$$

For small errors and for the values of coupling characteristic of the side-coupled accelerator structures which have been built at Los Alamos, the effects of $\hat{M}_D$, $\lambda\hat{E}$, and $\lambda\hat{F}$ are small compared with that of $\hat{M}$. Thus if only the most significant terms are retained either in (12) for the case without direct coupling or in (13) under condition (14) for the case with direct coupling, there results

$$\hat{M}\vec{\delta X} - A_P\lambda_P\hat{E}\vec{X}_P = \lambda_P\vec{\delta X}.$$

Thus, to first order, the error analysis without direct coupling is the same as with direct coupling, and the first order results previously derived for the former case[2] can be directly applied to the latter. It is to be noted, however, that while for the case without direct coupling, the errors ϵ_n are with respect to the intended uniform cell frequency ω_i; for the case with direct coupling, (or the case with near-neighbor coupling variations) the errors ϵ_n are with respect to the adjusted cell frequencies ω_{an} satisfying condition (14). This similarity of behavior with or without direct coupling for the equivalent error conditions has been observed many times in the digital computer "experiments", which are further described in the sections to follow. For tuning errors of 0.1 percent or less, the shunt impedance calculated with direct coupling differs from the shunt impedance without direct coupling by less than different runs (with different errors) under either condition differ among themselves.

Circuit Analog "Experiments" By Digital Computer

The analog circuit equations (see (3) above) are simple enough that they may be solved directly on a digital computer. Thus it is possible to run an "experiment" by computer, wherein the behavior of the analog is investigated for a given operating condition. The effects of errors in tuning or in other parameters are being investigated in this manner, using a random number subroutine to generate errors within any desired limits. The equations are solved by a matrix diagonalization process. By taking advantage of the fact that the original matrix has at most 5 non-zero elements in any row, and that the matrix is nearly symmetrical, the required memory space for the whole set of equation coefficients is reduced to approximately 4N complex numbers, rather than the approximately NxN complex numbers implied at first glance by (3). Thus very long accelerator models may be analyzed. Direct solution of the circuit equations is being used for investigating such items as the effect of increasing the coupling at the drive cell, the effect of having a temperature gradient along a chain of cavities, or tank, and the effect of coupling several tanks together to form one long chain of cavities with multiple drives.

Effect of Increasing the Coupling at the Drive

If the drive to a waveguide section is placed in a cell bridging the quadrupole focusing and mechanical coupling assembly between two accelerator sections, the field in the bridge is not used for acceleration, and the local configuration of fields at the drive point has no direct interaction with the beam. (See Fig. 2.) The coupling from the drive cell into the adjacent coupling cells may thus be adjusted to suit the designer. Calculations have been made for the case in which the coupling at the drive cell is twice the nearest-neighbor coupling at other cells. The effect of this increase of the coupling at the drive is to change the shape of the mode spectrum and the drive impedance vs. frequency variation only at the ends of the spectrum, leaving the behavior near the $\pi/2$ mode unchanged. (See Fig. 3 and 4.) The sensitivity to tuning errors is, for all practical purposes, unchanged. These results appear valid whether direct coupling is present or not.

Effect of a Temperature Gradient Along a Chain of Cavities

An alternative to using power splitters to feed a multi-section accelerator module from one drive is to use resonant cavities to bridge the gaps as in Fig. 5. This possible alternative raises the question if one cooling system is used, different sections may be at slightly different

temperatures. In the operation of a chain of cavities consisting of 4 sections and one drive, for example, one or two sections may be above the average temperature (and correspondingly lower in frequency), but if other sections are correspondingly lower in temperature (higher in frequency), the whole chain, or tank, may still appear to resonate at the correct frequency at the drive point. A series of calculations was performed to investigate the extent that the performance might be affected by such a temperature tilt in a tank consisting of 4 sections with 24 main cells each. Direct coupling between main cells or between coupling cells was not considered here. It was assumed that bridge cavities with increased coupling to the adjacent coupling cavities were used to join the sections. The assembly was assumed to be driven in the center bridge cavity, as in Fig. 5 (b).

When the temperature shifts of the sections were symmetrical around the drive (e.g., sections 1 and 4 set 20 kHz below sections 2 and 3), no significant change in effective shunt impedance from the case without temperature shifts was observed. In another calculation, the sections 1 to 4 were assumed to be 30 kHz low, 10 kHz low, 10 kHz high, and 30 kHz high, respectively, corresponding to running the cooling water in only one direction along the chain of cavities with a water temperature rise of approximately 5°C. This temperature tilt lowered the shunt impedance by about 2 percent or less from the no-tilt case. (Cooling water is normally run in both directions along a chain, thus producing a much smaller temperature tilt.) The main cell tuning errors were 100 kHz or less and the coupling cell tuning errors, 200 kHz or less for the above calculations. Some typical results for larger error limits are listed in Table I.

It appears that temperature control tolerances may be relaxed considerably, perhaps a factor of 10, if the sections of a drive module are thus coupled together and operated and cooled as one unit.

Table I

Example of Calculated Shunt Impedance of a Module With Four Sections Relative to the Case With No Tuning Errors and No Temperature Shifts

Error Limits		Relative Shunt Impedance		
R_1	R_2	Case A	Case B	Case C
100 kHz	200 kHz	0.9941	0.9947	0.9807
200	400	0.9874	0.9883	0.9729
300	600	0.9792	0.9816	0.9634

R_1 = error limit for main cell tuning errors (errors may be plus or minus)

R_2 = error limit for coupling cell tuning errors

Case A: No temperature tilts.
Case B: Sections 1 and 4 shifted 20 kHz lower than sections 2 and 3.
Case C: Sections shifted as follows: +30, +10, -10, -30 kHz.

For all the above cases: near neighbor coupling, 4.2%, direct coupling, 0; near neighbor coupling at ends of bridge cavities, 8.4%; main cell Q, 24,000; coupling cell Q, 12,000; operating frequency, 805 MHz; syncronous phase, 26°.

Effect of Coupling Chains Together to Form a Long Chain With Multiple Drives

If the many chains of cavities in a long linear accelerator could be electrically coupled together to make one long chain, the problem of controlling the phase of the drives to produce the correct phase for acceleration throughout the structure would be made simpler. Some new problems would be introduced however. One such question that arises is: How much more sensitive to tuning errors is a long structure with multiple drives as compared to an equivalent structure with the sections operated independently? The circuit analog is presently being used to investigate this question.

With a given set of tuning errors, the impedances seen at the several drives will not in general be all at the resonance point. Consequently, the calculation assumes that the section of cells being fed by each drive is raised or lowered together in frequency as a block until the impedance is entirely resistive at each drive. This corresponds to changing the cooling water temperature of the various sections so as to match the impedance at the various drives simultaneously. This is done in the circuit analog calculation by using a Gaussian least squares procedure to estimate the frequency changes to be applied to each section to simultaneously reduce the reactive components of all drive impedances to zero. Examples of the variation of the cell response amplitude and phase along such a long chain of resonators are shown in Fig. 6 and 7. In the case shown, main and coupling cell tuning error limits were 100 and 200 kHz respectively, and no direct coupling was assumed. The section lengths correspond to those of modules 29 to 36 of the Los Alamos tentative 800 MHz accelerator layout of Nov. 1, 1965. The shunt impedance for the particular set of tuning errors for this case was not found to be significantly different whether the 8 sections were operated independently or as one chain.

It can be seen from Fig. 7 that while the phases of the responses of the main cells are very near to 0 degrees or 180 degrees (as they should be for acceleration), the phases of the coupling cells may fall anywhere in the range 0 to 360 degrees, depending upon the nearby main cell tuning errors. As predicted by the perturbation theory,[5] the observed behavior of the circuit model is affected little by tuning errors in the coupling cells until such errors become enormously large.

Further investigation of the long tank with multiple drives is necessary to determine whether it is truly feasible from the electrical viewpoint. It is hoped to extend the current calculation methods to treat tanks with more than 8 drives and to determine the effects of variations along the structure of other parameters, such as coupling constants and Q.

References

1. T. Nishikawa, S. Giordano, and D. Carter, "Dispersion Relation and Frequency Characteristics of Alternating Periodic Structure for Linear Accelerators", Rev. Sci. Instr., Vol. 37, No. 5 (May 1966), p. 652-661.

2. T. Nishikawa, "Normal Mode Analysis of Standing Wave Linacs - Field Excitation and Beam Loading in Linac Cavities", Brookhaven AADD-87, BNL-9833, Nov. 15, 1965. (Unpublished).

3. J. M. Potter, "The Mode Spectrum of an Infinitely Long Biperiodic Chain of Doubly Coupled Resonators", LASL MP-3/JMP-1, Sept. 30, 1965 (Unpublished); also J. P. Blewett, "Network Representation of $\pi/2$ Mode Accelerating Waveguide System", Brookhaven AADD-65, BNL-8914, Feb. 8, 1965 (Unpublished).

4. G. R. Swain, "Notes on Tuning a Chain of Doubly Coupled Resonators", LASL MP-3/GRS-2, May 1966 (Unpublished).

5. D. E. Nagle, "Coupled Resonator Model of Linear Accelerator Tanks", Proc. MURA Conf. on Linear Accelerators, Stoughton, Wis., July 20-24, 1964; MURA-714, p. 21-30, Available from U.S. Dept. of Commerce, Springfield, Va. TID-4500.

   E. A. Knapp, "800 Mev RF Structures", Proc. MURA Conf. on Linear Accelerators, op. cit., p. 31-59.

   E. A. Knapp and B. C. Knapp, "Experimental Checks on the Validity of the Coupled Circuit Approximation for a Chain of Coupled Resonators", LASL P-11/EAK/BCK-1, Aug. 4, 1964 (Unpublished).

   D. Nagle, B. Knapp, and E. Knapp, "Perturbation Theory for the Doubly Periodic Chain", LASL P-11/DN/BK/EK-1, Dec. 1, 1964 (Unpublished).

6. B. C. Knapp, E. A. Knapp, G. J. Lucas, and J. M. Potter, "Resonantly Coupled Accelerating Structures for High-Current Proton Linacs", IEEE Trans. Nuclear Science, Vol. NS-12, No. 3 (June 1965), p. 159-165.

   R. A. Jameson, "Envelope Response of a Chain of Coupled Circuits", LASL P-11/RAJ-3, June 1, 1964 (Unpublished).

   R. A. Jameson, "Transient Response of a Chain of Coupled Circuits", LASL P-11/RAJ-4, June 22, 1964 (Unpublished).

7. R. L. Gluckstern, "Equivalent Circuits for Cavity Chains", LASL MP-4/RLG-4, Aug. 19, 1965 (Unpublished); "Coupling Elements in Equivalent Circuit for Cavity Cells", Brookhaven AADD-90, Aug. 20, 1965 (Unpublished).

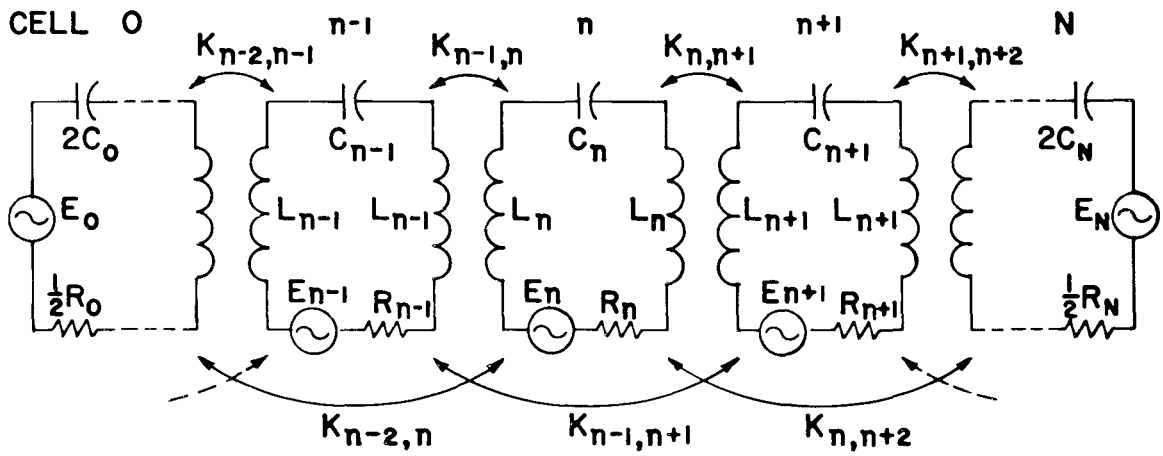

Fig. 1. General circuit analog for a chain of N+1 cavities. Magnetic coupling between neighboring resonators is indicated at the top of the figure; magnetic coupling between next-nearest resonators, at the bottom.

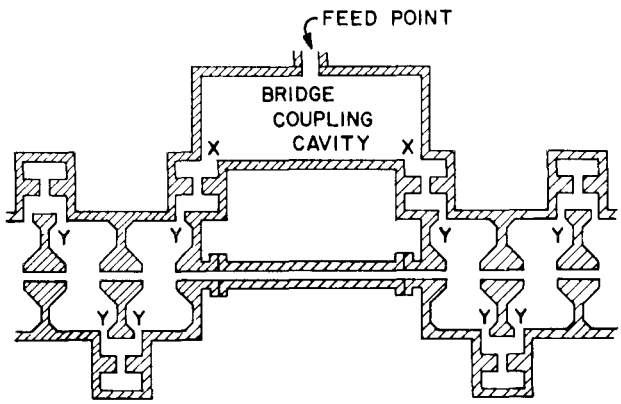

Fig. 2. Sketch of resonant coupling cavity bridging the gap between accelerator sections. The coupling between cavities at X may be larger than at Y.

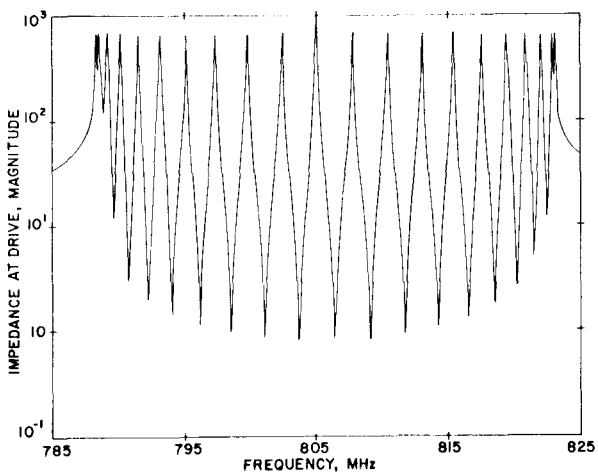

Fig. 3. Sketch illustrating type of variation of impedance at drive with frequency when coupling is uniform.

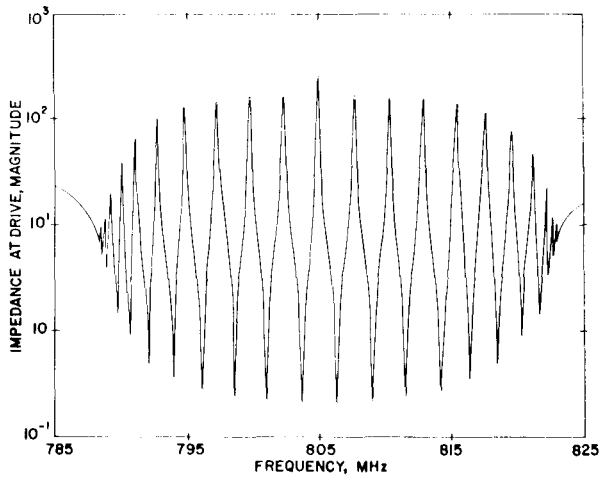

Fig. 4. Sketch illustrating type of variation of impedance at drive with frequency when coupling between drive cell and adjacent cells is doubled.

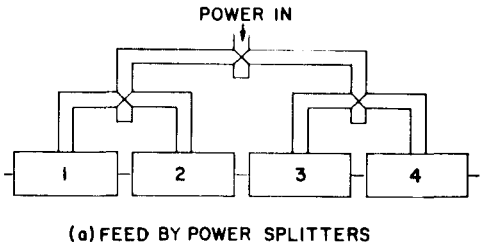

Fig. 5. Alternative methods of feeding an accelerator module consisting of 4 sections. Each section is a chain of coupled cavities.

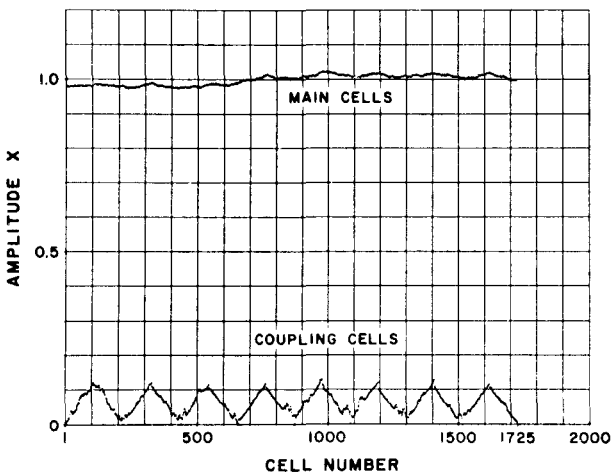

Fig. 6. Calculated amplitude X versus cell number for a long tank with 8 drives, 4.3 ± 0.0043 percent near neighbor coupling, no direct coupling, main cell Q increasing from 22,300 for section 1 to 23,000 for section 8, coupling cell Q 11,000; and main and coupling cell tuning error limits, 100 and 200 kHz, respectively.

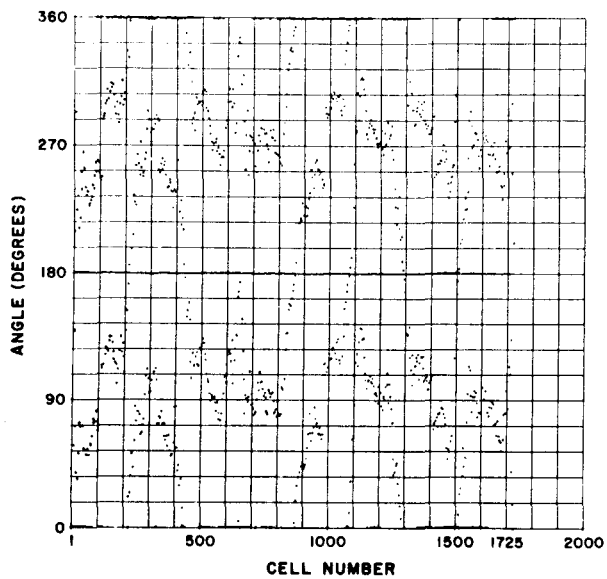

Fig. 7. Calculated cell phase versus cell number under the same conditions as in Fig. 6.